PULSED LASER DEPOSITION OF $BaCe_{0.85}Y_{0.15}O_3$ FILMS

F.W.Dynys* and A. Sayir#
*NASA-GRC, 21000 Brookpark Rd., Cleveland, OH 44135, USA
NASA-GRC/CWRU, 21000 Brookpark Rd., Cleveland, OH 44135, USA

ABSTRACT

Pulsed laser deposition has been used to grow nanostructured $BaCe_{0.85}Y_{0.15}O_{3-\delta}$ films. The objective is to enhance protonic conduction by reduction of membrane thickness. Sintered samples and laser targets were prepared by sintering $BaCe_{0.85}Y_{0.15}O_{3-\delta}$ powders derived by solid state synthesis. Films 2 to 6 μm thick were deposited by KrF excimer laser on Si and porous Al_2O_3 substrates. Nanocrystalline films were fabricated at deposition temperatures of 600-800 ^oC at O_2 pressure of 30 mTorr and laser fluence of 1.2 J/cm^2. Films were characterized by x-ray diffraction, scanning electron microscopy and electrical impedance spectroscopy. Dense single phase $BaCe_{0.85}Y_{0.15}O_{3-\delta}$ films with a columnar growth morphology is observed, preferred crystal growth was found to be dependent upon deposition temperature and substrate type. Electrical conductivity of bulk samples produced by solid state sintering and thin film samples were measured over a temperature range of 100 ^oC to 900 ^oC in moist argon. Electrical conduction of the fabricated films was 1 to 4 orders of magnitude lower than the sintered bulk samples. With respect to the film growth direction, activation energy for electrical conduction is 3 times higher in the perpendicular direction than the parallel direction.

INTRODUCTION

Metal oxides with the perovskite structure are one of the most versatile classes of solid materials known. The structure can accommodate a wide range of cations and exhibit a variety of conductivity behavior ranging from predominantly electronic to purely ionic. Structure can accommodate distortions of the ideal cubic structure which provides the capability to incorporate cations of different sizes, tolerate vacancy formation and tolerate atomic-scale intergrowths with other structural motif. High temperature protonic conduction in perovskite based ceramics, $BaCeO_3$ and $SrCeO_3$, was discovered by Iwahara et al.[1] The general formula of these materials is ABO_3, with A being a divalent earth alkaline element like Ba or Sr and B being a tetravalent element like Ti, Zr or Ce. A trivalent dopant element like Y, Yb or Gd is partially substituted on the B site to enhance protonic transport. Charge neutrality is maintained by oxygen vacancies that can be filled by hydroxyl groups. These materials exhibit dominant proton transport at temperatures up around 800°C. Protonic transport have been investigated in numerous ABO_3 type compositions: $A(B'_xB''_{1-x})O_{3-\delta}$, $(A'_xA''_{1-x})BO_{3-\delta}$, $(A'_xA''_{1-x})(B'_xB''_{1-x})O_{3-\delta}$, $A_2(B'_xB''_{1-x})O_{6-\delta}$ and $A_3(B'_{2+x}B''_{2-x})O_{9-\delta}$. High temperature protonic conductors (HTPC) have potential applications as electrolytes in fuel cells, gas sensors, gas purification systems and steam electrolyzers.

Combining high protonic conductivity with thermodynamic stability is considered to be a key problem for HTPC materials for electrochemical applications. Hydrogen permeation rate for HTPC materials has been found to be inversely proportional to membrane thickness.[2] Thus, reduction in HTPC membrane thickness is a practical approach to enhance the hydrogen permeation rate. To fabricate thin HTPC membranes on the order of 25 μm, they have to be supported using porous structures to provide mechanical strength. Successful processing of inexpensive membranes fabricated by particle deposition methods is hindered by high sintering

temperatures that exceed 1500 ^{o}C.[3] Reaction between the substrate and HTPC membrane is a processing problem. Pulsed laser deposition (PLD) is ideally suited to investigate protonic conductivity of perovskite films because the complex target composition can be reproduced at the substrate. The ease with which the stoichiometry of a multi-component system can be maintained in the deposited films is a significant advantage for PLD over other conventional physical vapour deposition techniques. PLD is being routinely used to deposit high quality, highly oriented thin films of multi-component oxide materials such as superconductors, ferroelectrics, ferrites, and biomaterials.[4] In the present paper, we report the deposition of $BaCe_{0.85}Y_{0.15}O_{3-\delta}$ and $(Ba_{0.9}Sr_{0.1})(Ce_{0.75}Y_{0.15}Ti_{0.1})O_{3-\delta}$ thin films by PLD. The films have been deposited on single crystal silicon wafers and porous Al_2O_3 substrates. The goal is to enhance protonic conduction by reduction of substrate thickness and utilization of nano-crystalline structures. Enhanced grain boundary conduction has been reported for nanocrystalline CeO_2 and Y_2O_3 stabilized ZrO_2 films.[5,6,7] Deposition temperatures ranging from 600 to 800 °C produced nano-crystalline films with columnar growth morphology. The influence of the processing parameters on the crystalline property and electrical conductivity are presented with a tentative interpretation of the results.

EXPERIMENTAL PROCEDURE

High-density $BaCe_{0.85}Y_{0.15}O_{3-\delta}$ (BCY) and $(Ba_{0.9}Sr_{0.1})(Ce_{0.75}Y_{0.15}Ti_{0.1})O_{3-\delta}$ targets/bulk samples were fabricated from powders synthesized by solid state reaction. Targets and bulk samples were sintered at 1650 ^{o}C. A previous paper describes the powder synthesis and sintering in more detail.[12] BCY films were grown in a stainless steel high vacuum chamber evacuated to a base pressure of 1x 10^{-6} Torr using a turbo molecular pump. A 248-nm KrF excimer pulsed-laser operated at 4 Hz, with an energy density of 1.2 J/cm2 was utilized to grow BCY films. The target was rotated around its axis to ensure uniform ablation, mounted at an angle of 45 ° to the laser beam and target surface parallel to the substrate surface. The laser beam was focused to a beam size of 4.2 cm^2 on the BCY target. Target to substrate distance varied from 100–130 mm. to attain sufficient interaction between the plasma plume and the process gas. Substrates were attached to a resistance heater; temperature was monitored by a thermocouple attached to the inner wall of the heater block. Substrate temperature was varied from 600 to 800 ^{o}C. Closed loop pressure control was used to maintain a chamber pressure of 30 mTorr using O_2 as the process gas. Single-crystal silicon wafers and porous Al_2O_3 substrates were used for thin film deposition. Porous Al_2O_3 substrates were prepared by pressing Biakowski A-10 powder into discs and sintering the disc at 1100 ^{o}C for 1 hr. No etch procedures were used to remove the thin SiO_2 surface layer on the silicon wafers. BCY films, 2 - 6 μm, were obtained using deposition times of 2 to 3 hrs. Film growth was approximately 0.05 nm/pulse. The as-grown films were cooled to room temperature at a rate of 5 ^{o}C/min at 30 mTorr of O_2. No failure of the BCY film was observed at this cooling rate. The crystalline structure of the as-deposited films was characterized by x-ray diffraction(XRD) and the microstructures examined by a scanning electron microscope(SEM). SEM and surface profilometer was used to determine the film thickness. The x-ray diffractometer was equipped with a Cu K_α source with a wavelength of 0.1540 nm. The operating conditions were 45 KV and 40 mA. Scans were conducted at 3^{o}/min with a sampling interval of 0.02^{o}.

The electrical properties as a function of the frequency of the material were determined with electrical impedance spectroscopy (EIS). Instrument combinations, Solartron 1260 impedance analyzer with Solartron 1287 electrochemical interface or Solartron 1260 with 1296 dielectric interface, were used to acquire impedance spectrum from 0.1 to 1 MHz. Platinum electrodes were used on bulk samples. Platinum paste (Heraeus CL11-5349) was applied to the sample surfaces and heat treated at 1050 ^{o}C for 1 hr. in air. Two thin film electrode geometries were utilized for EIS measurement as shown in figure 1. This provided a method to evaluate protonic conductivity parallel and perpendicular to the film growth direction. Bottom and top electrodes of Au/Pd film, ~ 100 nm, were deposited on silicon and BCY film by sputtering as illustrated in Figure 1. Non-coated areas on the samples were achieved by physical masking. Ag electrodes on porous Al_2O_3 substrates were fabricated from Ag paste and heat treated at 300 ^{o}C for 0.5 hr. in air. No special proton loading treatment was performed prior to sample testing. The samples were placed into a ProboStat (NorECs Norwegian Electro Ceramics AS) test fixture that is equipped with a closed end alumina process tube. The vertically mounted process tube is aligned in a vertical tube furnace. Pt wire was adhered to electrodes by using Pt paste or Ag paste to complete the circuit connections. Atmosphere of argon or air was used in testing. Moist atmosphere was obtained by using a Nafion membrane. Measurement temperature ranged from room temperature to 900 ^{o}C, temperature control of the specimen was ±2°C. The EIS measurement was control by a computer using Labview software (National Instruments Corp.). The sample was allowed to equilibrate with temperature and atmosphere for 1 hr. before testing.

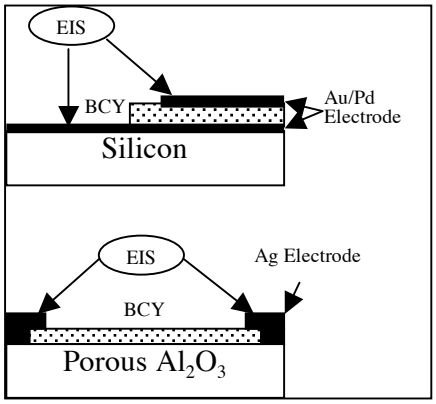

Figure 1. BCY film geometries for EIS measurement.

RESULTS AND DISCUSSION

The microstructure and properties of films are strongly dependent on the deposition process. The phase purity and the orientation of the deposited films were examined by x-ray diffraction. Analysis of XRD patterns showed that the orientation is dependent on deposition temperature and substrate material. No secondary phase formation was detected from XRD anaylsis for the deposited BCY films. In comparison, CeO_2 formation has been observed for magnetron sputtered $BaCe_{0.9}Y_{0.1}O_{3-\delta}$ films as reported by He et al.[8]. Figure 2 shows the crystalline nature of $(Ba_{0.9}Sr_{0.1})(Ce_{0.75}Y_{0.15}Ti_{0.1})O_{3-\delta}$ films deposited on silicon at room temperature, 600 ^{o}C and 800 ^{o}C. In Figure 2, Silicon peaks are identified, the unmarked peaks are $(Ba_{0.9}Sr_{0.1})(Ce_{0.75}Y_{0.15}Ti_{0.1})O_{3-\delta}$. Amorphous film is produce at room temperature deposition. At 600 ^{0}C, the large peak at 41.45^{o} indicates a preferentially oriented film along the (400) plane. It is not unusual for polycrystalline films to exhibit a preferential orientation when deposited on single crystalline substrates. A more random crystal orientation is obtained at 800 ^{o}C. The Sr and Ti doping produces a XRD pattern that matches well with the ICCD data for $BaCeO_{3-\delta}$ (00-022-0074). Figure 3 shows SEM photographs of $(Ba_{0.9}Sr_{0.1})(Ce_{0.75}Y_{0.15}Ti_{0.1})O_{3-\delta}$ film grown at 800 ^{o}C. Figure 3B shows a fracture surface exposing the film cross-section. Growth of columnar grains is observed. The grains form a dense film. Nanosized grains are observed as shown in Figure 3A. Grains are rectangular shaped with a grain size ≤ 100 nm.

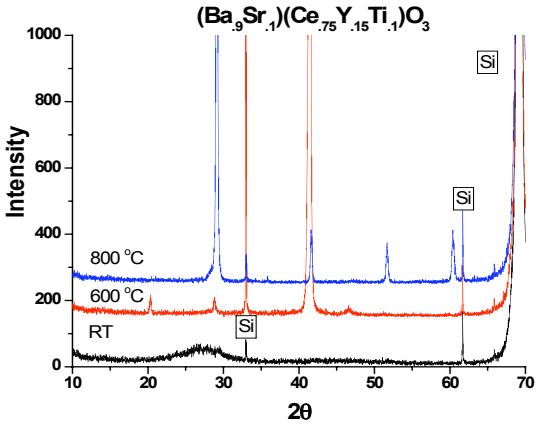

Figure 2. XRD patterns of $(Ba_{0.9}Sr_{0.1})(Ce_{0.75}Y_{0.15}Ti_{0.1})O_3$ films deposited on silicon substrates at rt, 600 °C and 800 °C at 30 mTorr of O_2

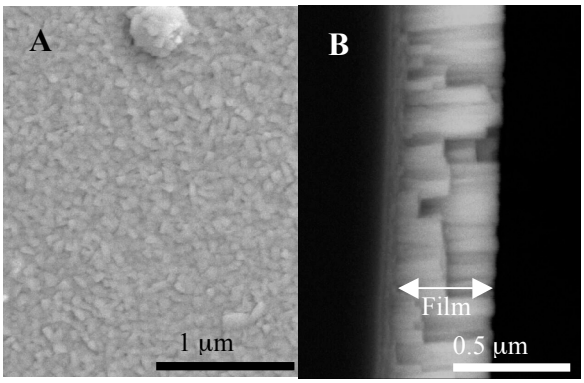

Figure 3. Microstructure of $(Ba_{0.9}Sr_{0.1})(Ce_{0.75}Y_{0.15}Ti_{0.1})O_3$ film deposited at 800 °C: (A) Film surface and (B) Film cross-section.

Figure 4 shows the crystalline nature of BCY films deposited on uncoated and Pt coated porous Al_2O_3 substrates at 800 °C. The coated substrate contained a Pt coating derived from Pt paste. The Al_2O_3 and Pt peaks are marked in Figure 4; the unmarked peaks are BCY. Both crystalline BCY films exhibit some preferential orientation as indicated by the large (400) peak. Figure 5 shows an SEM photograph of BCY film grown over a porous Al_2O_3 substrate at 800 °C. The SEM image is a fracture surface exposing the film cross section.. A distinct interface is observed between the BCY film and porous substrate. Dense films can be grown over the porous substrate. The crystalline BCY film has a columnar-like growth structure, the columns are not as well defined as observed for the growth structure on single crystal silicon. The rough surface topography and random Al_2O_3 crystal orientation can contribute to this specific growth structure.

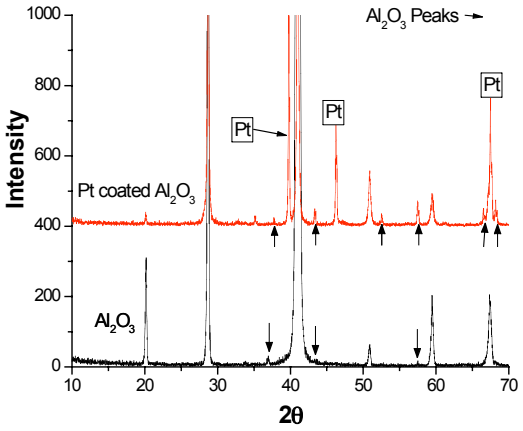

Figure 4. XRD patterns of $BaCe_{0.85}Y_{0.15}O_3$ films deposited on porous Al_2O_3 substrate and Pt coated substrate.

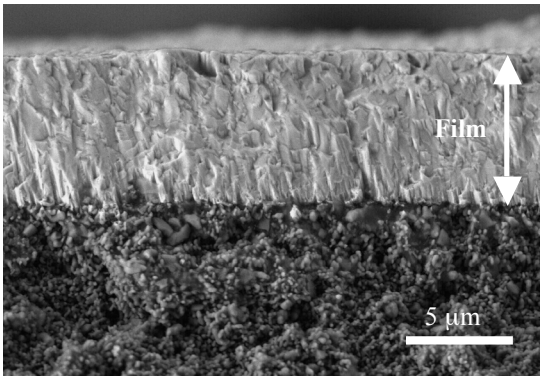

Figure 5. Microstructure of $BaCe_{0.85}Y_{0.15}O_3$ film deposited on a porous Al_2O_3 substrate.

The electrical properties of the bulk and thin film samples were measured by EIS. A series of representative spectra over the complete temperature range are shown on a Nyquist plots in Figure 6. A humidified argon atmosphere with a dew point of 25 °C was utilized for

testing. At low temperatures, two distinct impedance arcs were observed up to 150 °C. The small arcs at the higher frequencies can be attributed to the response of grain interiors, while the larger arcs can be attributed to the response of grain boundaries. Only one arc is observed at higher temperatures indicating that bulk and grain boundary responses are indistinguishable. As the temperature is increased, the resistance decreases and the time constants *(RC)* of the relaxations associated with polarizations are reduced shifting the arcs to higher frequencies.

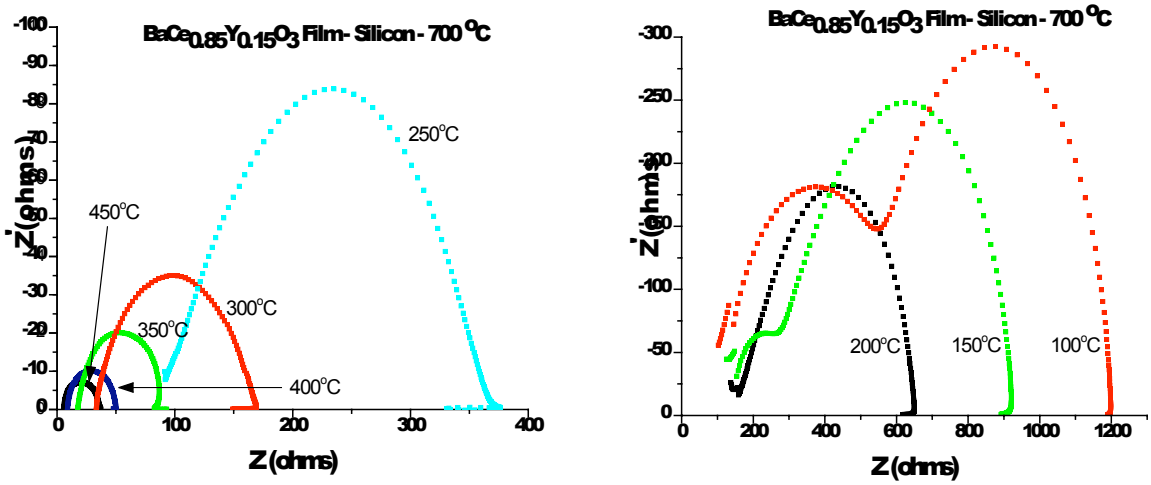

Figure 6. Temperature dependent impedance spectrum of $BaCe_{0.85}Y_{0.15}O_3$ film deposited on silicon at 700 °C.

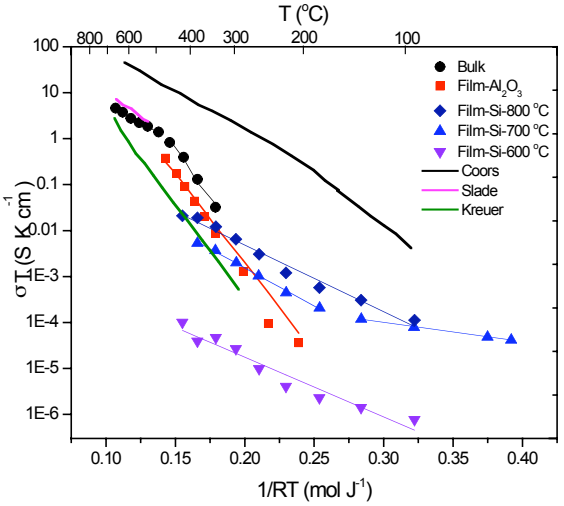

Figure 7. Conductivity plot comparing the results of this work with results from the published literature by Coors and Readey, Slade and Singh, and Kreuer..

The complex impedance plots were analyzed by fitting with different equivalent circuits to obtain the resistance and capacitance of different arcs at different temperatures. The total conductivities were calculated from the total resistance. Sample geometry was used to determine the conductance. The equivalent circuit $(RQ)_{Grain}(RQ)_{GrainBoundary}(R)_{electrode}$, where R = resistance and Q = constant phase element or CPE, was used to model the impedance spectrum. Circuit parameters for the equivalent circuits were obtained by using the least squares fitting routine in Zview (Scribner Aossiciates).

The apparent energies for electrical conduction, Q, were determined by plotting $\sigma \cdot T$ vs 1/RT using the Arrhenius equation of $\sigma \cdot T = A \cdot \exp(-Q/RT)$. Figure 7 is plot of the electrical conduction along with published results for bulk $BaCe_{0.9}Y_{0.1}O_3$ and $BaZr_{0.9}Y_{0.1}O_3$ film. The data in is fitted by least square analysis to provide the activation energies for electrical conduction. Table 1 lists the calculated Q values and pre-exponential values for samples measured. Published data for bulk $BaCe_{0.9}Y_{0.1}O_3$[9,10] and

$BaZr_{0.9}Y_{0.1}O_3$ film[11] is included in Table 1. The sintered sample exhibits the highest electrical conductivity compared to the PLD fabricated thin film samples. Sintered specimen shows an apparent change in electrical conduction behavior above and below 550 °C. A Q value of 100.3 KJ/mol is calculated for the low temperature electrical conduction and 38.57 KJ/mol for the high temperature electrical conduction. The change in electrical conduction behavior cannot be elucidated from the present data. XRD data from sintered specimens exhibit second phase formation during sintering as shown in Figure 8.[12] The arrows in Figure 8 mark unidentified XRD peaks for BCY sintered at 1650 °C for 4 hrs. The powder XRD pattern is also shown to illustrate single phase material prior to sintering Phase formation appears to inhibit electrical conduction at low temperatures. Further work is needed to characterize the sintered samples. High temperature electrical conduction data is compatible with Slade and Singh's data but an order of magnitude lower than Coors and Readey's data. High temperature Q value is lower than reported for $BaCe_{0.9}Y_{0.1}O_3$: 44.2 and 48.9 KJ/mol.

Table 1
Activation Energy

	Temp. (°C)	Activation Energy (KJ/mol)	Pre-exponential (SK/cm)
$BaCe_{0.85}Y_{0.15}O_3$ Bulk	600 - 850 400 - 550	38.6 100.3	275.61 2.15×10^6
Porous Al_2O_3	150 - 600	89.1	1.06×10^5
Si – 800 °C	100 - 500	33.4	3.86
Si – 700 °C	200 – 500 25 - 150	38.2 9.6	3.2 1.8×10^{-3}
Si – 600 °C	100 – 500	29.9	6.87×10^{-3}
Coors/Readey $BaCe_{0.9}Y_{0.1}O_3$	100 - 900	44.24	9.2×10^3
Kreuer $BaZr_{0.9}Y_{0.1}O_3$	350 - 900	93.1	4.88×10^4
Slade/Singh $BaCe_{0.9}Y_{0.1}O_3$	600-900	48.9	1.38×10^3

Figure 7 indicates that the electrical conduction for thin films exhibits dependence upon deposition temperature and type of substrate. Further work is needed to establish the dependence because the film thickness was not held constant. It has been shown in the literature that electrical conduction is also dependent upon film thickness. The BCY film thicknesses on the silicon wafers were 3.4 μm, 6.0 μm and 6.0 μm for deposition temperatures of 600 °C, 700 °C and 800 °C, respectively. The results show that BCY film on silicon exhibits the highest electrical conduction at a deposition temperature of 800 °C. Calculated activation energies are 33.4, 38.2 and 29.9 KJ/mol for BCY films deposited at 600 °C, 700 °C and 800 °C, respectively. These values are somewhat lowered than the bulk samples, 38.57 – 48.96 KJ/mol. It should be noted that the low temperature data for BCY film deposited at 700 °C indicates a change in conduction behavior below 150 °C. Activation energy of 9.2 KJ/mol was calculated for temperature regime of 48 °C to 150 °C. Further measurements are needed to confirm this result.

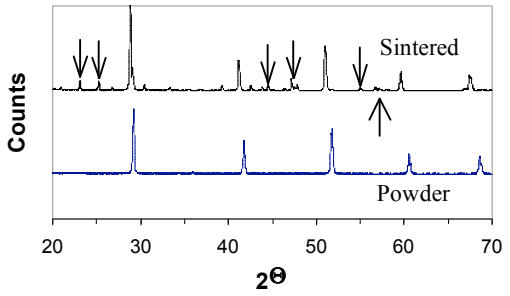

Figure 8. XRD patterns of BCY sintered at 1650 °C for 4 hrs. and synthesized BCY

Conduction behavior of BCY film deposited upon a porous Al_2O_3 substrate exhibits different temperature dependence than the BCY films deposited on silicon as shown in Figure 7. The Q value for the BCY film on porous Al_2O_3 is 89.1 KJ/mol, this 2.3 to 2.9 times larger than the Q values for BCY films on silicon. However, the Q value complements the low temperature Q values for the bulk sample and Kreuer's data on $BaZr_{0.9}Y_{0.1}O_3$ film. It should be noted that the

measured BCY film thickness is 3.4 μm and 6 μm for the $BaZr_{0.9}Y_{0.1}O_3$ film. The measurement was made perpendicular to the film growth direction. It is not proven if the measurement is directional dependent for films or a microstructural related variable that is controlling the low temperature electrical conduction. Since the Q values are similar between bulk and thin film, one might expect second phase material being the problem.

Based on the results, the electrical conductivity of the HTPC materials are not a singular function of composition and phase content. Further work is required to elucidate the microstructural contribution. Specifically, the contribution of grain versus grain boundary phases. Partitioning of cations between these phases impacts vacancy formation and ordering. Isolating these contributions will help devise a material with enhanced protonic conduction.

SUMMARY

Temperature dependent protonic conduction was measured in BCY sintered samples and BCY films by EIS in a moist argon atmosphere. BCY films were fabricated on silicon wafers and porous Al_2O_3 substrates by PLD. Dense nano-crystalline films with columnar growth morphology were deposited at 600 ^oC to 800 ^oC at 30 mTorr of O_2. Preferential growth orientation is favored at lower deposition temperatures. All BCY films exhibit a lower total electrical conduction than the sintered specimens by 1 to 4 orders of magnitude. Total electrical conductivity followed Arrhenius behavior. Activation energy for electrical conduction for the sintered specimens was 38.57 KJ/mol at temperatures $\geq$600 ^oC and 100.3 KJ/mol at temperatures <600 ^oC. BCY films deposited on silicon exhibit similar activation energy, 29.92 to 38.8 KJ/mol, to the high temperature bulk data. BCY film deposited on porous Al_2O_3 exhibited activation energy of 89.1 KJ/mol, similar to the Q value for low temperature bulk sample.

ACKNOWLEDGEMENTS

Financial support for this work was obtained from NASA Glenn Research Center, Brookpark, Ohio under cooperative agreement NCC3-850 through Internal Research and Development Program.

REFERENCES

[1] H. Iwahar et al., Solid State Ionics, 11, 1983, 109.
[2] S. Hamakawa et al., Solid State Ionics 48, 2002, 71.
[3] K.D. Kreuer et al., Solid State Ionics 145, 2001, 295.
[4] D. E. Chrisey (Ed.), *Pulsed Laser Deposition of Thin Films*, John Wiley & Sons, N.Y., 1994.
[5] I. Kosacki et al., Electrochem Soc., Proc., 97**,** 1998, 631.
[6] T. Suzuki et al., J. Am. Ceram. Soc., 84**,** 2001, 2007.
[7] H.L. Tuller, Solid State Ionics 131, 2000, 143.
[8] T. He et al., Solid State Ionics 89, 1996, 9.
[9] C. T. Slade and N. Singh, Solid State Ionics, 46, 1991, 111.
[10] W.G. Coors and D.W. Readey, J. Am. Ceram. Soc*.,* 85, 2002, 2637.
[11] K.D. Kreuer, Ann. Rev. of Mat. Res., 33, 2003, 333.
[12] F. Dynys et al., p. 293, *Cer. Eng. & Sci. Proc.*, 25(3), E. Lara-Curzio and M.J. Readey (Ed.), American Ceramic Society,Westerville, OH, 2004.